Experimental Study to Investigate the Flow Pattern Associated to Angled Groins

Ibrahim M. M.

Shoubra Faculty of Engineering, Benha University P.O. box 11629, Shoubra, Egypt
mohamed.ibrahim@feng.bu.edu.eg

Abstract: Groins (spur dikes) are structures constructed at an angle to the flow in order to deflect the flowing water away from critical zones. The main objectives of the study are to investigate the hydrodynamic impact of oriented groin existence in a stream bed. A 2-D laboratory flume model was used. About 30 runs were carried out for monitoring the impact of groin length, orientation angle, and the discharge on working length, and velocity components. 28 measuring points were used for velocity measurements distributed as 4 lines from A to D crossed by 7 cross sections. The study showed that the straight groin of 8cm (20% contraction ratio) has the longest working length, however the repelling groin of angle of 60^0 and 4cm length of (10% contraction ratio) presented the shortest working length. The velocity was decreased than the basic case at the nearest velocity line to groin installation; however the velocity increased than the basic case for the rest lines. The velocity was inversely proportional to groin length upstream and downstream groin location. The impact of groin orientation angle on velocity was exclusive at lines A and B; however the impact was vanished after that at lines C and D. Groin installation proved high efficiency in bank protection especially with high discharges
[Ibrahim M. M **Experimental Study to Investigate the Flow Pattern Associated to Angled Groins**] *J Am Sci* 2012;8(10):313-322]. (ISSN: 1545-1003). http://www.jofamericanscience.org. 46

Key Words: Groins; Flume Model; Contraction Ratio; Orientation Angle; Working length; Hydrodynamic Impact.

1. Introduction

Groins are the most common structures involved in problems of bank erosion, in addition to acting as river training works used to regulate rivers. They have been recognized as hydraulic structures extending outward from the bank of stream to deflect or attract the flow. For the purposes of bank protection against erosion, reduce the velocity of flow along river banks owing to their roughness, maintenance of navigation channels, in addition to control flow into or out of a bend through meandering channel (Mohamed, 2002).

For economic reasons, groins are often constructed of riprap and are commonly designed to be submerged during high flows. Despite the widespread use of groins, many aspects of their design are based on prior experience and are only applicable to streams of a similar nature. Copeland, (1983) recommended that groins should be oriented either normal to the flow or slightly downstream for best performance. Mayerle et al. (1995) developed 3-D numerical model including a module of changing turbulent viscosity for flow simulation in the vicinity of spur dikes. The model was based on the solution of the time dependant nonlinear Navier Stokes equations, kinematic condition of the free surface, and the continuity equations respectively for the velocities in the horizontal plane, the surface elevation, and the vertical velocity. Most of previous studies concerning the velocity profile in vicinity of groins were involved in cases of groins installed at right angles to bank, however the flow pattern around more angles is still rare. Therefore, this research is focusing on detailed velocity measurements and working length around oriented groins.

2. The Experimental Work

The experimental work was carried out in the laboratory of the hydraulics research Institute (HRI) of the National Water Research Center, Delta Barrage. The used flume has a rectangular cross section with overall length 40.0 m, width of 0.4 m and 0.6 m deep. The side walls along the entire length of the flume are made of glass with wood-frames. The horizontal bottom of the flume was made of ceramics and wood. The water entered the flume from a pump which feeds the flume with a max. discharge of 30 l/s. The flume is associated with a steel wooden gate with an orifice with a rectangular shape, also has movable downstream gate is located at the end of the flume.

3. Measuring Devices

One ultrasonic flow-meter with an accuracy of + 1% were used to determine the discharge. It was installed on a 16" diameter feeding pipe. The flow velocities were measured using an Electro-Magnetic current-meter type E.M.S. (manufactured by Delft Hydraulics). The device was connected to a mean value meter to show the average velocity within a selected time period.

To monitor the water levels, two point gauges with side stilling wells were installed. Also, a mobile point gauge with an accuracy of + 0.1 mm was used to measure the water and bed level. Video and photo cameras were also essential to record the flow patterns in vicinity the groin field.

Figure1: General View of the Used Flume

4. Model Runs

A comprehensive test program was thus selected to cover the different flow conditions and operation of the flume Table (1). The flow conditions were carried out at different contraction ratio (the ratio between groin length (L), and flume width (W)) 0.1, 0.15 and 0.2. The discharge was varied as 10, 20, and 30 l/s. Also, the orientation angles were varied (the inclined angle between the groin and the flow direction) 60, 90, and 120 degree. (Figure 2) The run names were formulated as symbol B refers to basic case, while the symbols N, S, and T refers to orientation angle in degrees Ninety, Sixty, and hundred Twenty, respectively. The first number refers to discharge in lit/s, while the subtitle number refers to percentage of contraction ratio. (e.g. $10N_{20}$ means groin of ninety degrees, 20% contraction ratio length, and 10 l/s discharge).

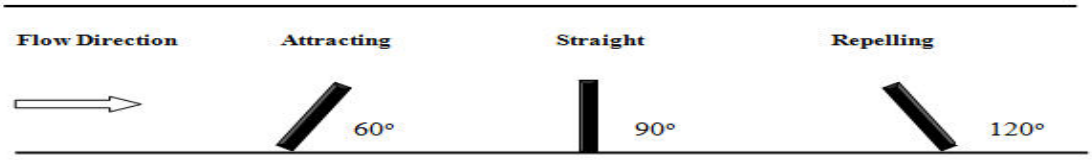

Figure 2: Shape of Oriented Groins According to Flow Direction

Table 1: Test Program and Run Names

RUN NO.	RUN NAME	Q (l/s)	L/W	Orientation Angle	Groin Position
1	10B	10	-------	-------	-------
2	20B	20			
3	30B	30			
4	$10N_{20}$	10	0.2	90	Straight
5	$20N_{20}$	20			
6	$30N_{20}$	30			
7	$10S_{20}$	10		60	Attracting
8	$20S_{20}$	20			
9	$30S_{20}$	30			
RUN NO.	**RUN NAME**	**Q (l/s)**	**L/W**	**Orientation Angle**	**Groin Position**
10	$10T_{20}$	10	0.2	120	Repelling
11	$20T_{20}$	20			
12	$30T_{20}$	30			
13	$10N_{15}$	10	0.15	90	Straight
14	$20N_{15}$	20			
15	$30N_{15}$	30			
16	$10S_{15}$	10		60	Attracting
17	$20S_{15}$	20			
18	$30S_{15}$	30			
19	$10T_{15}$	10		120	Repelling
20	$20T_{15}$	20			
21	$30T_{15}$	30			
22	$10N_{10}$	10	0.1	90	Straight
23	$20N_{10}$	20			
24	$30N_{10}$	30			
25	$10S_{10}$	10		60	Attracting
26	$20S_{10}$	20			
27	$30S_{10}$	30			
28	$10T_{10}$	10		120	Repelling
29	$20T_{10}$	20			
30	$30T_{10}$	30			

5. Study Results and Analysis

5.1. The Working Length

It's defined as the summation of separation point length (S.P.) and the reattachment point length (R.P.); the separation point length is located at the tip or just upstream the groins. However the reattachment length is defined as the point where the flow pattern reattaches to the river main flow in the downstream direction, (Attia and El Said, 2006). The working lengths are measured in flume through pouring a colored liquid in the flow upstream groin then measure the length of reverse current upstream and downstream to be separation point and the reattachment point lengths respectively.

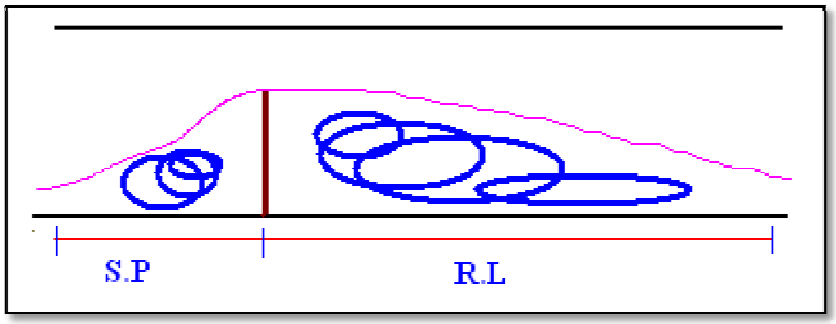

Figure 3: Flow Pattern around Groin

Table 2: The Working Length

RUN NAME	S.P (m) Length	R.P (m) Length	Working length (m)	Working length As a Function of (L)
10B	-------	-------	-------	-------
20B				
30B				
$10N_{20}$	0.880	0.410	1.290	16.13
$20N_{20}$	0.400	1.460	1.860	23.25
$30N_{20}$	0.530	3.160	3.690	46.13
$10S_{20}$	0.555	0.259	0.814	10.18
$20S_{20}$	0.250	0.925	1.175	14.69
RUN NAME	S.P (m) Length	R.P (m) Length	Working length (m)	Working length As a Function of (L)
$30S_{20}$	0.330	2.000	2.330	29.13
$10T_{20}$	0.750	0.350	1.100	13.75
$20T_{20}$	0.340	1.250	1.590	19.88
$30T_{20}$	0.450	2.700	3.150	39.38
$10N_{15}$	0.070	0.850	0.920	15.33
$20N_{15}$	0.150	0.950	1.100	18.33
$30N_{15}$	0.230	1.500	1.730	28.83
$10S_{15}$	0.060	0.810	0.870	14.50
$20S_{15}$	0.100	0.870	0.970	16.17
$30S_{15}$	0.170	1.200	1.370	22.83
$10T_{15}$	0.060	0.440	0.500	8.33
$20T_{15}$	0.190	0.950	1.140	19.00
$30T_{15}$	0.215	1.500	1.715	28.58
$10N_{10}$	0.060	0.540	0.600	15.00
$20N_{10}$	0.135	0.755	0.890	22.25
$30N_{10}$	0.190	1.300	1.490	37.25
$10S_{10}$	0.045	0.330	0.375	9.38
$20S_{10}$	0.080	0.625	0.705	17.63
$30S_{10}$	0.110	0.900	1.010	25.25
$10T_{10}$	0.035	0.300	0.335	8.38
$20T_{10}$	0.080	0.650	0.730	18.25
$30T_{10}$	0.130	0.850	0.980	24.50

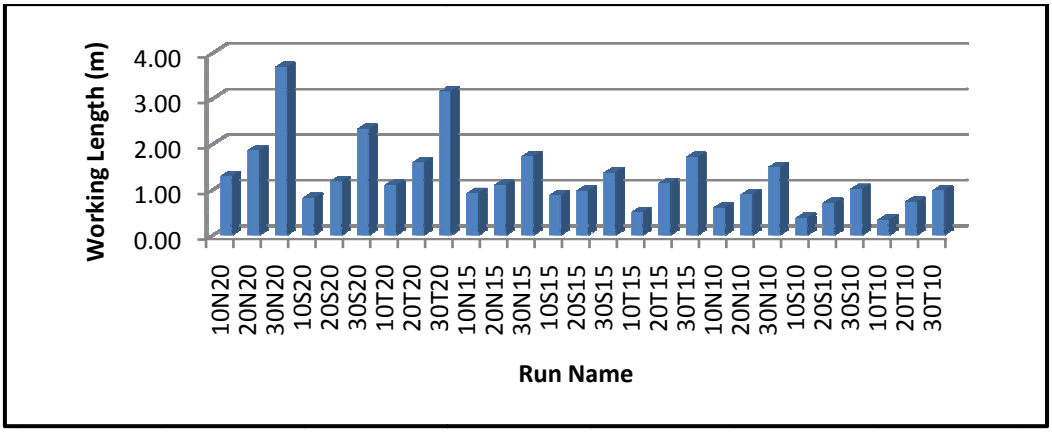

Figure 4: The Working Length for the Tested Cases

Combining table2, and figure 4, it's concluded that the maximum working length was found at groin of 8cm length (20% contraction ratio), 90 degrees (straight spur), and 30 l/s discharge. That was due to under a fixed length, the straight spur decreases the flume width when compared to attracting and repelling groins. This in turn restricts a larger amount of flow upstream, the velocity at groin tip increase, and consequently the working length increases too.

Moreover, it's noticed that the repelling groin shows longer working length when compared to the attracting groin under same conditions. That is due to the attracting groin has lower values for the separation point lengths when compared to the straight and the repelling groins which is well noticed in table2. Also, the same results were found when presenting the working length as a product of groin length.

5.1.1. Impact of Orientation Angles and Contraction Ratio on Working Length

Figure 5 illustrates the relation between the working length and the discharge for the tested orientation angles. The figure shows that under fixed groin length and discharge, the straight groin has the peak values for working length for the tested discharges. However, the attracting groin has the lowest ones. That differs with the results reported by Attia and El Said, 2006 as they mentioned that the repelling groin have the maximum working length.

Figure 6 shows the relation between the working length and the discharge for different contraction ratios. It's noticed that under fixed orientation angle and discharge, the working length is directly proportional to groin length. That agrees with what obtained by Attia and El Said, 2006.

Combining between figures 5 and 6 it was found that the working length is directly proportional to the discharge under fixed groin length and orientation angle.

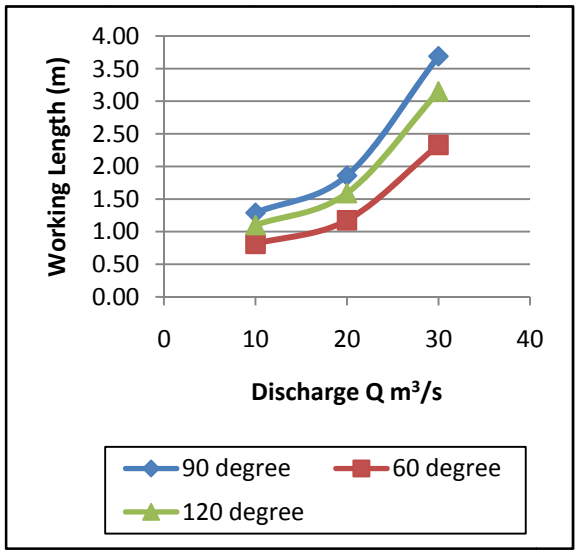

Figure 5: Impact of Orientation Angles on Working Length

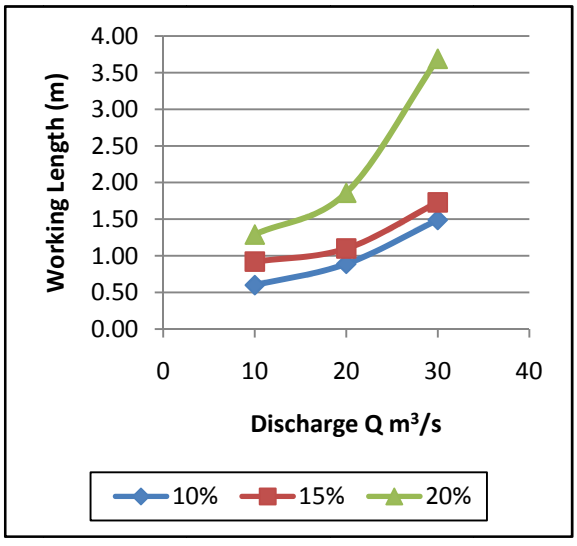

Figure 6: Impact of Contraction Ratio on Working Length

5.2. The Velocity Components

Doubtless, the velocity plays an important role which considered the back bone to define the functional properties for the tested groins.

The locations of velocity measurement are carefully selected to cover the groin field. A mesh consists of 28 measuring node distributed in 4 lines A, B, C, and D crossed by 7 cross sections were used. 12 nodes of 28 are distributed too close to groin to investigate the local impact for groin implementation. However the rest 16 nodes are distributed quietly far from groin location to define its impact on velocity profile over a long distance. (Figure 7)

It should be mentioned that the 7 cross sections covers 2m to distributed as 0.25m upstream groin location and 1.75m downstream where the repelling length is much shorter than the reattachment length. The mentioned distances were selected after studying the working length as the distance of 2m between the first and last cross sections covers 90% of the tested cases. (Table 2 and Figure 4)

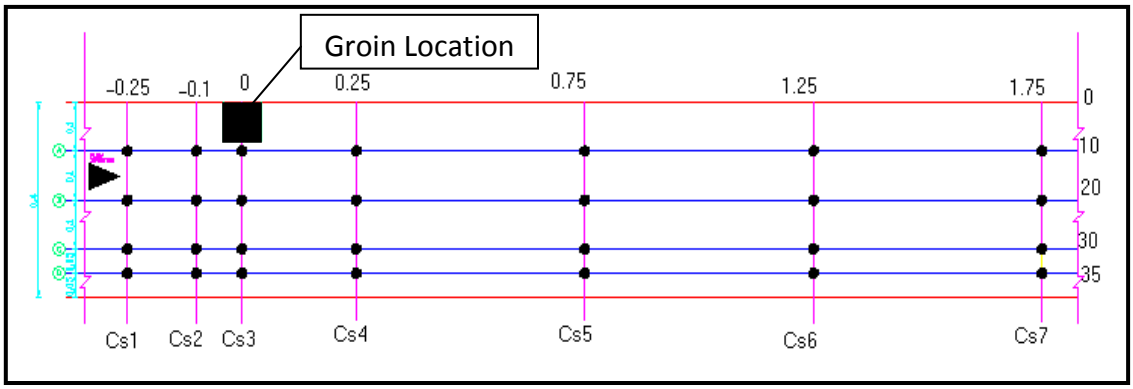

Figure 7: The Location of Velocity Measurement Nodes

To assure that groin installation shows a considerable impact on velocity in 3-D; figures 8 and 9 were plotted to illustrate the comparison in velocities at line A (the nearest line to groin location) between the basic case where no groins were installed and for $30N_{20.}$

The Run of $30N_{20}$ was selected as it presented the maximum working length; so it's expected that this run shows the maximum noticed impact in velocity distribution. The 3-D velocities were measured at 0.2, 0.6, and 0.8 from water depth.

The selected cross sections in figure 9 were chosen after carefully study for all cross sections, as cross section No.1 presents the beginning of groin field, and cross section No.3 presents the impact at groin location; however cross section No.7 presents the end of groin field.

From figures it's noticed that the maximum impact for groin existence located at cross section 4 directly downstream groin location. Moreover from the view of 3-D velocities, groin installation shows the extreme difference at 60% from water depth at groin location.

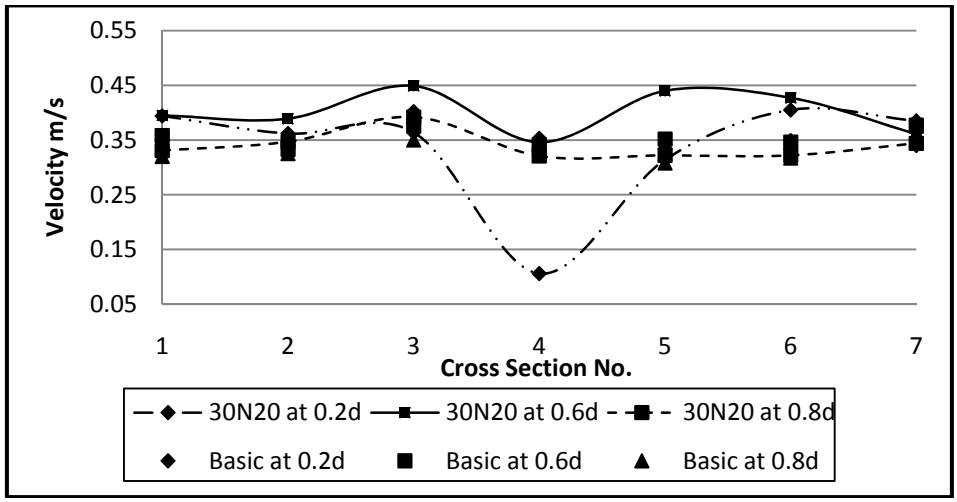

Figure 8: The Velocity Distribution at Line A for Basic Case and $30N_{20}$

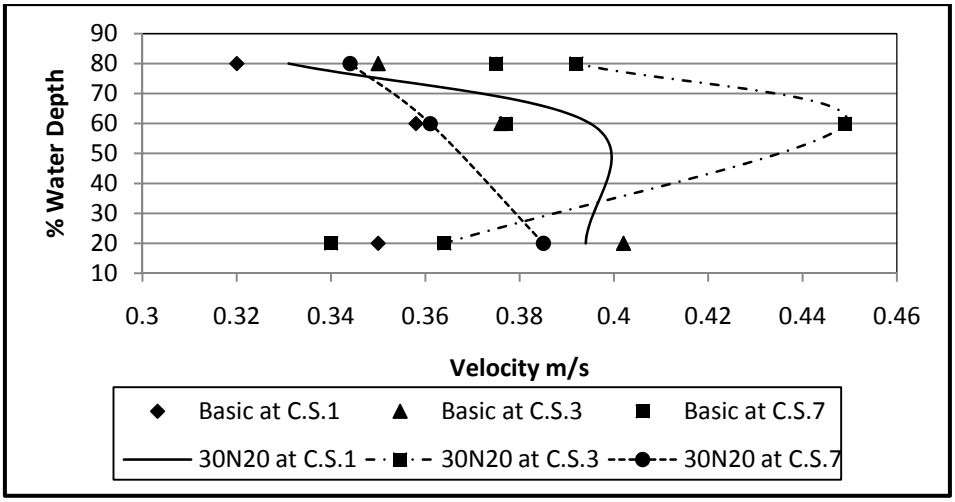

Figure 9: The 3D Velocity Distribution at the Intersection of Line A and Cross Sections 1, 3, and 7 for the Basic Case and $30N_{20}$

5.2.1. Impact of groin installation on different velocity lines

After proving the considerable impact of groin erection at line A in the previous section; the requirements to investigate its effect on the next velocity lines became heavy needed. Figure 10, illustrates the velocity distribution at 60% of water depth for different velocity lines. The comparison was between the basic case and 30 N_{20}. It's noticed that in case of no groin, lines A and D shows the same trend almost coincide on each other. Also, the same notice was found at Lines B and C. On the other hand, after groin erection, line A was the most influenced line due to groin existence, as it's fluctuated between 3 peaks. The greatest one was located at the cross section where the groin installed. Moreover, line A is the only one at which the velocity was decreased in both upstream and downstream groin location. Lines B and C show the same trend with different velocity values 12% ± 2% higher values than the basic case upstream groin and 27% ± 2% downstream. At line D, it's noticed that it has the same trend of line (A) upstream groin; however at downstream the situation was different as it has higher values with low fluctuations. From the figure it's concluded that groin installation decreases the velocity upstream and downstream at line (A), however it increases the velocity values at the rest velocity lines.

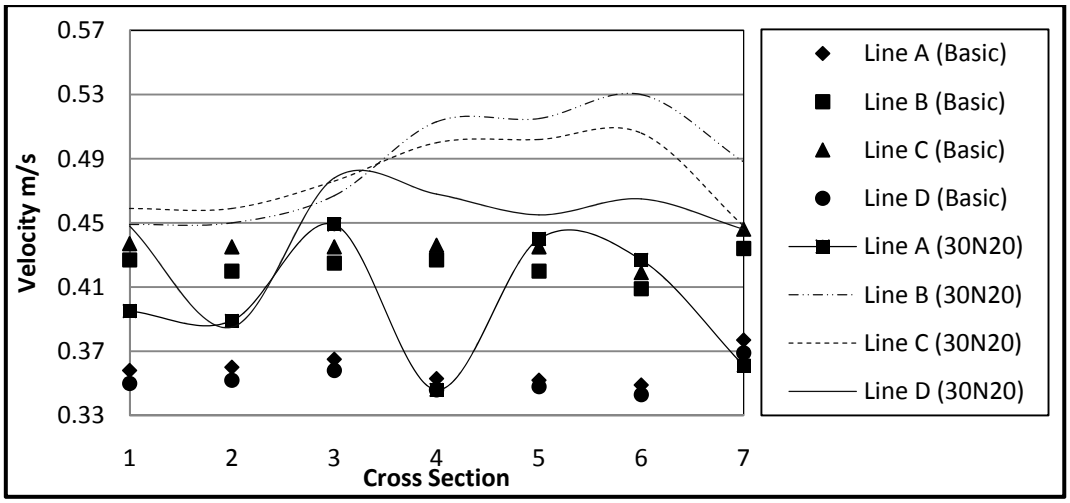

Figure 10: Velocity Distribution for the Basic Case and $30N_{20}$ at different Velocity Lines

5.2.2. Impact of groin length at different velocity lines

To investigate the relationship between groin length and velocity, figure 11 was plotted. The figure shows that at cross section 3, installing groin with any tested length shows the same impact on velocity which is higher than the basic case by 24% for groins with 4 and 6cm, while using groin with 8cm increases the velocity by 30%. Therefore, it's concluded that groin installation shows a good performance in deepen the navigation channels. Also, the figure illustrates that except at groin

location; the groin length was inversely proportional to velocity.

For the other velocity lines (B, C, and D) it's noticed that all tested lengths showed the same performance with slight higher velocity values for longer groins. Also it should be mentioned that at line D the velocity increased by 40% than the basic case at the cross section 3 where the groin was erected. Therefore, using groins acts as two edge weapon in bank protection at the side of groin construction and preventing deposition in the opposite side.

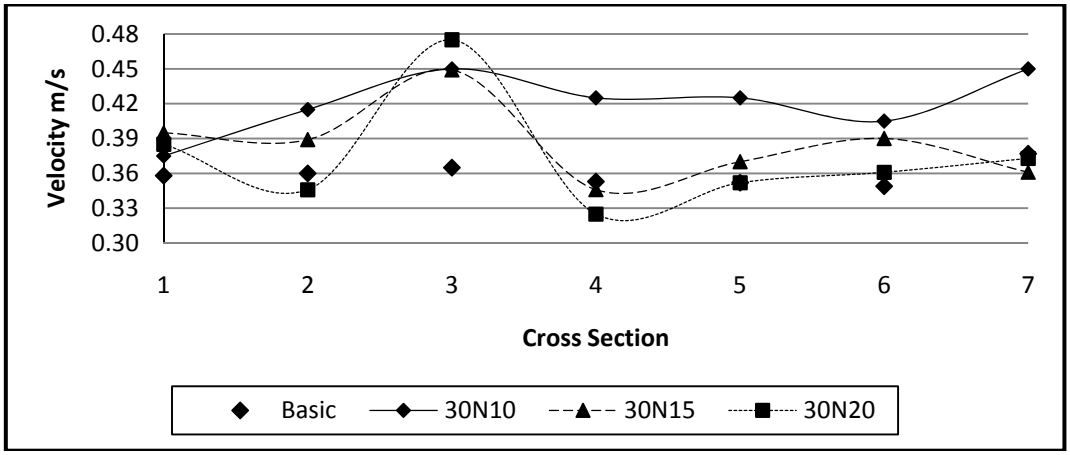

Figure 11: Velocity Distribution at Line (A) and 0.6d for Straight Groin with Different Lengths

5.2.3. Impact of groin orientation angle at different velocity lines

The velocity distribution in this section is analyzed only at lines A, and B; while lines C, and D it was found that groin existence shows no considerable effect. Figures 12, 13 show the velocity distribution for the tested angles at lines A and B respectively. The figures were plotted at 0.2d as it presents a noticeable variance in velocity values. However, groin length and discharge remained constants with maximum values 20% contraction ratio and 30L/s respectively. From figures investigations it's noticed that groin installation at any angle shows the same trend at all velocity lines but with different values. At line (A) the velocity due to groin existence at all sections was round the corresponding values for the basic case, while it decreased by three times than the basic case at cross section 4, just downstream groin location. Moreover, at cross section 4, the straight groin presents the maximum velocity depression while the repelling groin showed a velocity value 79% higher that the straight one. Hence, using straight groin is considered the best from the view of bank protection. At line B, using repelling and attracting groins increases the velocity than the basic case upstream in addition to downstream. On the other hand the straight groin presents the nearest values to the basic case. That means the morphological changes associated to straight groin existence are local and focused on groin tip. Consequently, installing straight groin is not efficient when used for increasing bed depth for navigational purposes in the mid channel away from groin location.

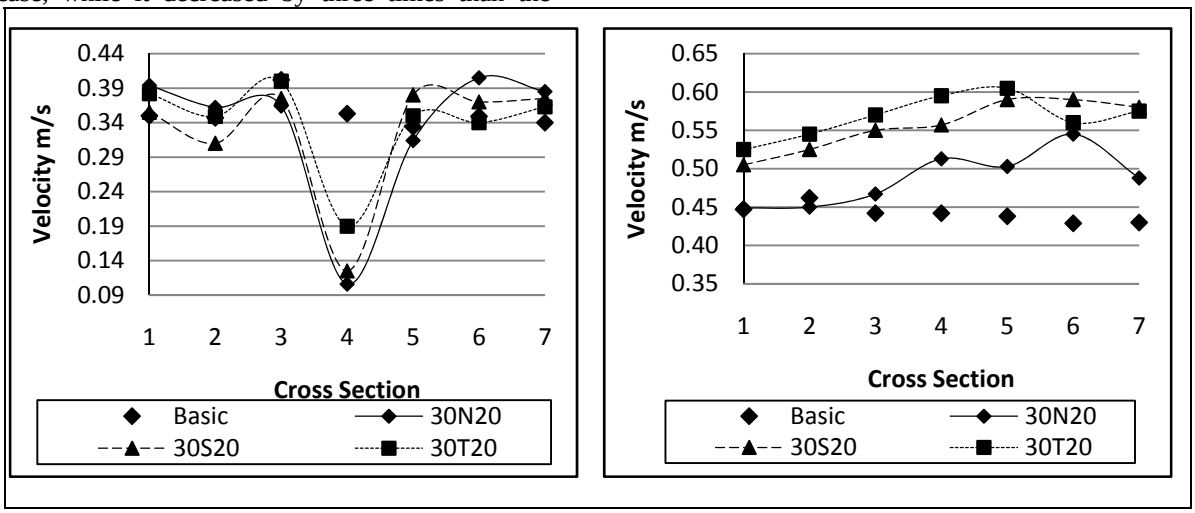

Figure 12: Velocity Distribution at 0.2d for Line (A)

Figure 13: Velocity Distribution at 0.2d for Line (B)

5.2.4. Impact of discharge at different velocity lines

Discharge is considered a focal parameter that affects the velocity distribution; according to continuity equation. Figure 14 was plotted to present the velocity distribution at line A at 0.2d with different discharges. Both groin length and orientation angle were fixed. The tested groin was selected to be straight (90^o) of 8cm length (20% contraction ratio). The figure illustrates that for the tested study cases, the same trend was found. The velocity decreased at cross section 4, directly downstream groin location, and then starts increasing again. The velocity decreased by 343.4% and 168.8% for discharge of 30 L/s. and 20L/s respectively when compared to the basic cases with same conditions.

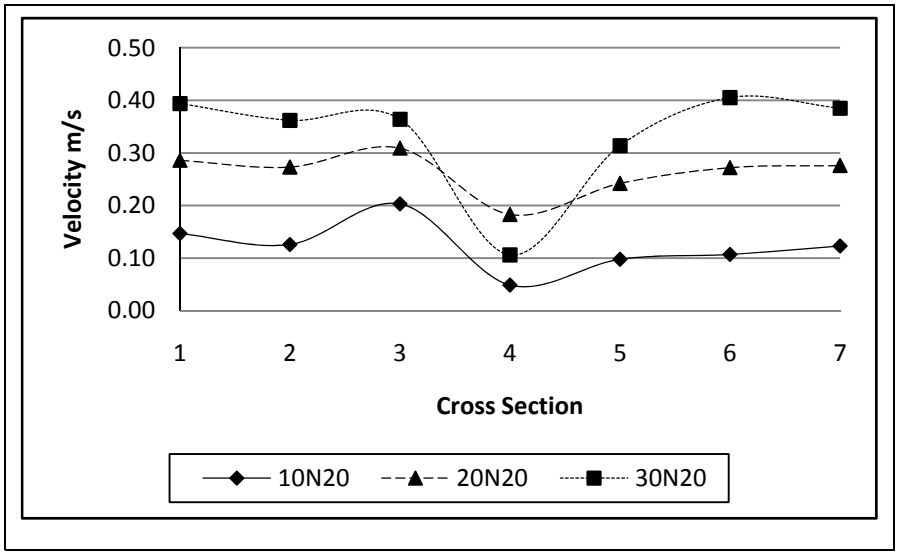

Figure 14: Velocity Distribution at Line (A) for Different Discharges

That assures the ability of groins to act as a bank protection structures under any discharge especially the high one. It should be mentioned that the impact of discharge at lines B, C, and D is small and inconsiderable.

Appendix (A) shows 2-D velocity distribution presented in form of contour maps and 3-D velocity distribution at line A for the basic case, $30S_{20}$, $30N_{20}$, and $30T_{20}$ respectively.

6. The Conclusions

The study cases concluded several remarks that emphasized the impact of oriented groins installed in straight open channel on working length and velocity components. Firstly, the working length, it's found that the peak values were located at straight groin, so it can be used effectively for bank protection purposes. The minimum values for working length were located at the attracting groin. Also, the working length was directly proportional to both discharge and groin length. Secondly, the velocity distribution, it's found that the nearest velocity line to groin erection is the most influenced one under the study cases, then the impact decreases towards the opposite bank. Moreover, the groin length was directly proportional to velocity at the cross section where the groin installed, however an inverse relationship was found between groin length and velocity just upstream and downstream groin location. The impact of orientation angle on velocity was only found at lines A and B. At line A, the velocity variance due to different angles was unnoticeable except at cross section 4 as the velocity was 3 times less than the basic case. While at line B, using groins at any specifications increasing the velocity. Also, it's found that the velocity was directly proportional to the discharge. Moreover, the study proved that groin installation shows a good performance with high discharges.

Appendix (A)

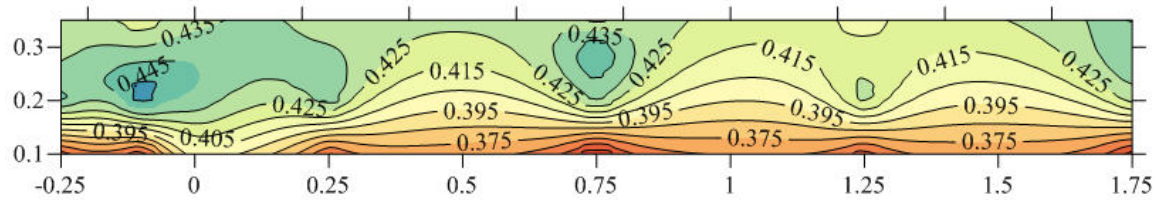

Figure A-1: 2-D Velocity Distribution for the Basic Case

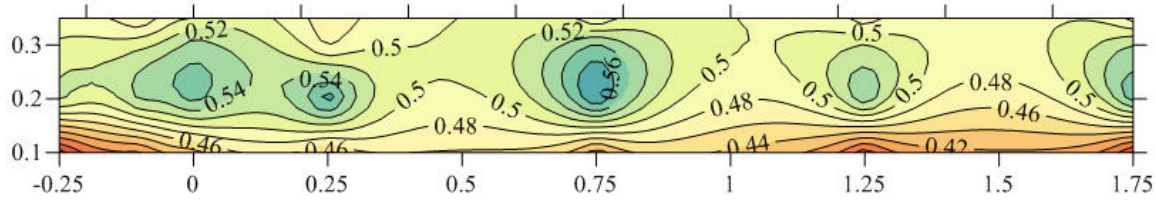

Figure A-2: 2-D Velocity Distribution for $30S_{20}$

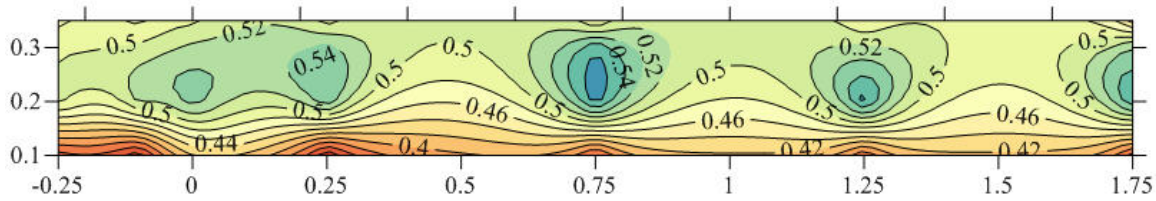

Figure A-3: 2-D Velocity Distribution for $30N_{20}$

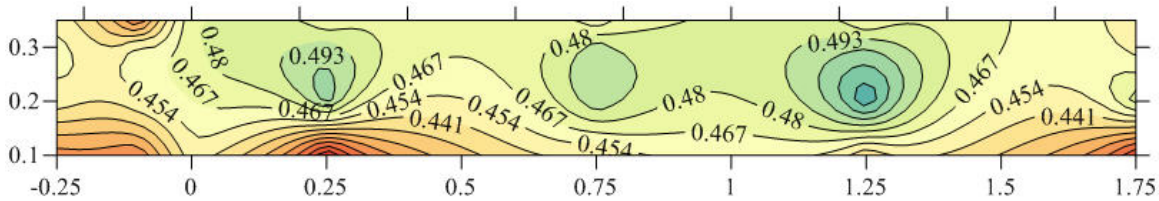

Figure A-4: 2-D Velocity Distribution for $30T_{20}$

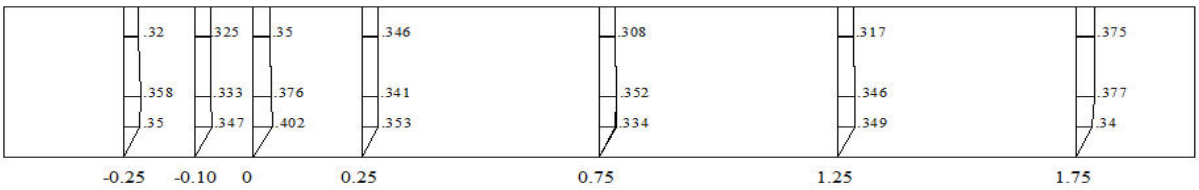

Figure A-5: 3-D Velocity Distribution at Line A for the Basic Case

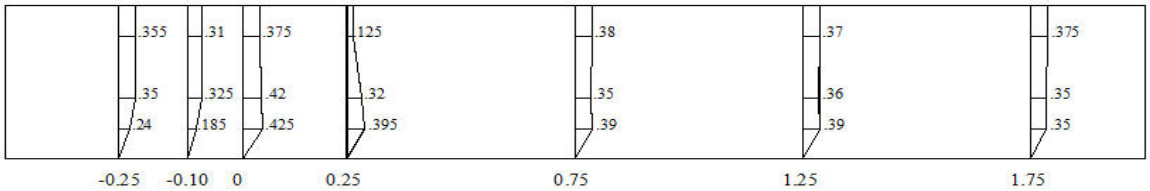

Figure A-6: 3-D Velocity Distribution at Line A for $30S_{20}$

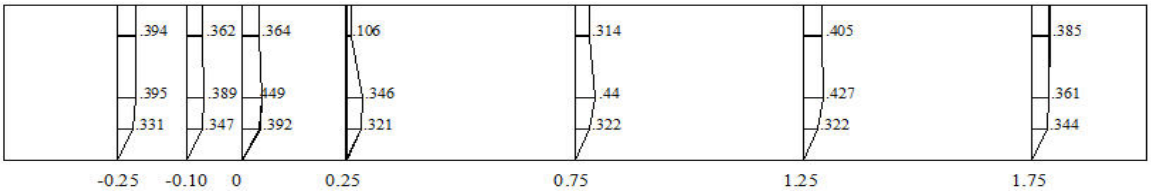

Figure A-7: 3-D Velocity Distribution at Line A for $30N_{20}$

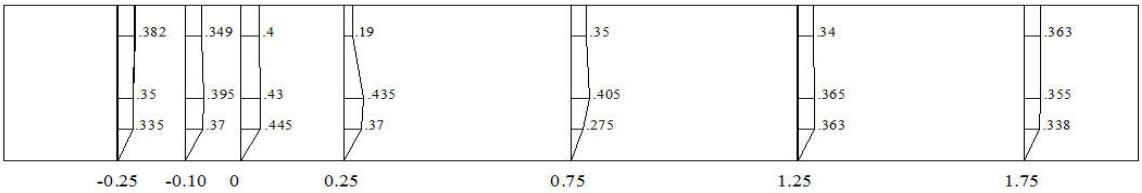

Figure A-8: 3-D Velocity Distribution at Line A for $30T_{20}$

Corresponding
Ibrahim M. M
Shoubra Faculty of Engineering, Benha University
P.O. box 11629, Shoubra, Egypt
mohamed.ibrahim@feng.bu.edu.eg

References

[1] Mohamed, M., Y.(2002): Thesis presented to Delft University of Technology, Netherlands, in Partial Fulfillment of the requirements for the Degree of Philosophy in Civil Engineering, 2002.
[2] Rajaratnam and Nwachukwu (1983): "Flow near groin-like structures." Journal of Hydraulic Engineering, ASCE, 109(3), 463-480.
[3] Attia, K. M., and El Said, G. (2006): "The Hydraulic Performance of Oriented Spur Dike Implementation in Open Channel" Paper presented to tenth international water technology conference, Egypt, 2006.
[4] Alvarez, J. A. M. (1989): "Design of Groins and Spur Dikes." Proceedings 1989 National Conference on Hydraulic Engineering, New Orleans, 296-301.
[5] Attia, K., M.(1996): Thesis presented to Ain Shams University, Egypt, in Partial Fulfillment of the requirements for the Degree of Philosophy in Civil Engineering, 1996.
[6] Mayerle, R., Toro, F. M., and Wang, S. S. Y. (1995): Verification of a Three Dimensional Numerical Model Simulation of the Flow in the Vicinity of Spur Dikes. Journal of Hydraulic Research, 33(2):81-88.
[7] Chen, F. Y., and Ikeda, S. (1997): "Horizontal Separation in Shallow Open Channels with Spur Dikes." Journal of Hydroscience and Hydraulic Engineering, 15(2): 15-30.
[8] Shields, F. D., Jr., Cooper, C. M., Knight, S. S., (1995). "Experiment in stream restoration."Journal of Hydraulic Engineering, ASCE, 121(6):494-502.
[9] Copeland, R. R., (1983). "Bank protection techniques using spur dikes." Miscellaneous Paper HL- 83-1, U. S. Army Waterways Experiment Station, Vicksburg, Mississippi, 32 pp.

9/2/2012